A&A 501, 375–380 (2009)
DOI: 10.1051/0004-6361/200810572

Astronomy & Astrophysics

ESO large program about transneptunian objects: surface variations on (47171) 1999 TC_{36}⋆

S. Protopapa[1], A. Alvarez-Candal[2], M. A. Barucci[2], G. P. Tozzi[3], S. Fornasier[2], A. Delsanti[2], and F. Merlin[2]

[1] Max-Planck-Institute for Solar System Research, Max-Planck-Str. 2, 37191 Katlenburg-Lindau, Germany
e-mail: protopapa@mps.mpg.de
[2] LESIA, Observatoire de Paris, 92195 Meudon Principal Cedex, France
[3] INAF, Osservatorio Astrofisico di Arcetri, Largo E. Fermi 5, 50125 Firenze, Italy

Received 11 July 2008 / Accepted 08 February 2009

ABSTRACT

Aims. We investigate the surface composition of the Plutino (47171) 1999 TC_{36}.
Methods. We completed near-infrared photometric and spectroscopic observations of (47171) 1999 TC_{36} with the adaptive optics instrument NACO at the ESO VLT during 12 October 2006, and present these data with ISAAC and SINFONI spectroscopic observations carried out about one month later on 9 November 2006 and 8 November 2006, respectively. The ISAAC and SINFONI spectroscopic observations were combined with a visible spectrum obtained by FORS1 on 9 November 2006. Composition and properties of the compounds present on the surface of the target are investigated by applying a Hapke radiative transfer model to the measured spectra and to previously published observations.
Results. We present the relative reflectance spectrum of (47171) 1999 TC_{36} in the wavelength range (0.37–2.33) μm. An intimate mixture of Triton tholin, Titan tholin, serpentine, and Triton tholin diluted in water ice represents the best-fit model description of the measured spectrum. Any significant differences from the published spectra of (47171) 1999 TC_{36} taken on 2001 and 2003 could be due to surface heterogeneity.

Key words. Kuiper Belt – techniques: spectroscopic – techniques: photometric – methods: numerical – scattering

1. Introduction

Scientific interest in understanding the physical properties of Transneptunian objects (TNOs) derives from the fact that they can provide important information about the origin and evolution of our Solar System. TNOs are considered the most pristine Solar System bodies, and the investigation of their surface composition can help constrain the global view of the early solar nebula at large distances from the Sun. Proposing to "unambiguously detect and quantify" all the compounds present on the surface of TNOs, a second ESO (European Southern Observatory) Large Program, with M.A. Barucci as principal investigator, has been accepted. In particular the main goal of this program is to acquire high signal-to-noise visible and near-infrared spectra for a large sample of TNOs, belonging to several dynamical groups. Detailed information about the composition of TNOs can be acquired from spectroscopic observations in the visible and near-infrared, where the most significant number of diagnostic absorption signatures can be found for this task. In the visible range, TNOs are characterized by mostly featureless spectra with different spectral gradients, ranging from neutral to very red. The red spectral gradient is generally associated with organic material on the surface of the body, such as tholins, which are the refractory residues of the irradiation of gases and ices containing hydrocarbons (Cruikshank et al. 2005). Different types of tholins have been studied, in particular Triton tholin and Titan tholin. They have been obtained by irradiating gaseous mixtures of nitrogen and methane, a lower CH_4 concentration existing in Triton tholin than in Titan tholin. The visible range is also important for detecting aqueous altered minerals (Lazzarin et al. 2003; Fornasier et al. 2004). The near-infrared spectral region (1–2.5) μm has proven to be the wavelength range containing the highest number of diagnostic signatures for the surface characterization of these objects, since ices, such as H_2O, CH_4, N_2, CO, and CO_2, have strong absorption bands in this region.

The analysis of the available TNO spectra have shown large variations in the spectral behaviour of these bodies, indicating the presence of four spectral groups into the Kuiper Belt: methane-dominated spectra, water-ice-dominated spectra, water-ice spectra with the presence of methanol-like features, and featureless spectra (Barucci et al. 2008). Large TNOs with diameter greater than 1300 km exhibit near-infrared spectra dominated by methane ice absorption bands (Brown 2008). Pluto (Olkin et al. 2007) together with Eris (Dumas et al. 2007), Sedna (Barucci et al. 2005), and 2005FY_9 [newly named Makemake] (Licandro et al. 2006; Brown et al. 2007a; Tegler et al. 2007, 2008) belong to this category. The only exception is 2003EL_{61} [newly named Haumea] (Trujillo et al. 2007; Brown et al. 2007b), which, although a large TNO, is a member of that group of objects characterized by water ice absorption bands. For this group, high quality spectra are necessary to distinguish between the objects with amorphous water ice from those, such as Charon (Brown & Calvin 2000) or Quaoar (Jewitt & Luu 2004), that exhibit the 1.65-μm feature, characteristics of crystalline water ice and important for the understanding of the physical processes occurring on TNOs. Several studies have been performed to explain how crystalline water ice could form at temperatures of 40–50 K and survive in spite of space weathering. Active

⋆ Based on observations at the European Southern Observatory, Chile within the framework of Program 178.C-0036.

Table 1. Characteristics of the spectroscopic observations of (47171) 1999 TC_{36} obtained at the ESO VLT.

Date	UT	Telescope	Instr.	airm	Solar An. (airm)	Seeing(″)
12 Oct. 2006	02:52	UT4 (Yepun)	NACO	1.11	HIP008455 (1.03)	1.5–1.6
8 Nov. 2006	01:20	UT4 (Yepun)	SINFONI	1.10	HD 2966 (1.06)	0.7–1.0
9 Nov. 2006	01:12	UT1 (Antu)	ISAAC	1.11	HD 2966 (1.02)	0.6–0.9
9 Nov. 2006	01:34	UT2 (Kueyen)	FORS1	1.08	HD 1368 (1.27)	0.8–1.0

Observational date, universal time (UT corresponding to the first target spectrum acquired), VLT unit and instrument used, airmass (mean of the airmass values at the beginning and the end of the target observation) and observed solar analog star with its airmass, used to remove the solar contribution, are reported. The visible wavelength seeing is listed. Spectroscopic observations acquired with FORS1 are discussed in detail in Alvarez-Candal et al. (2008).

crystallization processes such as impact or cryovolcanic outgassing on TNOs (Jewitt & Luu 2004) have been hypothesized, while Zheng et al. (2008) showed that the persistence of crystalline water ice in the outer region of the Solar System can be explained in terms of balance between the thermal recrystallization and irradiation-induced amorphization. The acquisition of high quality spectra is important also for the detection of the 2.27-μm feature related with the presence of methanol, found on TNOs such as 55638 2002 VE_{95} (Barucci et al. 2006) and maybe easily masked by the low signal precision of the available spectroscopic observations in the K-band. High signal-to-noise observations are required for the analysis of TNOs with featureless spectra to understand whether these objects really exhibit spectra resembling those of dead comets and jovian Trojans or whether they have to be placed into other groups.

Belonging to the group of TNOs with spectra characterized by water ice absorption bands is the Plutino (47171) 1999 TC_{36}, discovered to be a binary system by Trujillo & Brown (2002) and spectroscopically studied by Dotto et al. (2003) and Merlin et al. (2005). In this paper, we present results from spectroscopic and photometric observations of (47171) 1999 TC_{36} performed at the ESO-VLT (Very Large Telescope), Chile, with three instruments, NACO, ISAAC, and SINFONI, with the goal of improving our knowledge of the surface composition of (47171) 1999 TC_{36}. The importance of this work is that observations are available for (47171) 1999 TC_{36} in different periods between 2001 and 2006, through which we can investigate the surface heterogeneity or a possible temporal evolution of the target. Both phenomena are important for the understanding of the formation and evolution of TNOs.

2. Observations and data reduction

We present near-infrared photometric and spectroscopic observations of (47171) 1999 TC_{36} obtained with the NACO instrument at the ESO VLT during 12 October 2006, together with ISAAC and SINFONI spectroscopic observations carried out about one month later on 9 November 2006 and 8 November 2006, respectively. All the presented observations refer to the unresolved binary system (47171) 1999 TC_{36}.

2.1. NACO observations

NACO spectroscopic observations were performed using the prism S27_P1 with the CutOff_2.5 μm filter and the 172 mas slit. Using the NACO prism S27_P1, we covered the complete wavelength range (1.1–1.7) μm with a spectral resolution of 30. GSC 0467700763 (RA = 00:57:10.442 Dec = –03:17:05.57) is the reference source used for the visible Adaptive Optics (AO) sensor of NACO. The minimum distance (6.71″) between the AO star and the target was obtained around 03:00UT. NACO observations were planned to ensure that the target was sufficiently close to a star to benefit from the AO correction and resolve the binary system. Unfortunately because of the poor seeing conditions, we could not close the AO loop (see Table 1), and had to work in the open loop instead. As a consequence, we achieved lower spatial resolution, which was insufficient to resolve the binary system, and a lower signal-to-noise ratio in the spectra, responsible for a degraded spectral quality. The usual A-B-B-A nodding (with some jitter) along the slit was applied when acquiring the observations. In particular, the NACO_spec_obs_AutoNodOnSlit template, which nods the telescope between two positions (A and B) along the slit, was used. In this way, infrared images can be pairwise subtracted with the object of interest located on distinct regions of the detector. Spectra of the nearby solar analog HIP008455 (G2V spectral type), recorded immediately after the target observations, were obtained to remove the telluric and solar features simultaneously from the target spectra (see Table 1), obtaining the relative reflectance spectrum of the target. Calibration star observations were acquired with similar sky conditions and identical instrument settings as those of the target. The usual data reduction procedures for infrared spectroscopy, consisting of background subtraction, flat-fielding, and ABBA spectra coaddition were applied. Particular attention was paid to wavelength calibration, generally achieved using calibration frames. Because of the absence of arc lamp spectra for calibrating the strongly non-linear dispersion of the prism, the comparison between the telluric features of the sky background and the transmission spectrum of the earth's atmosphere over Kitt Peak (Hinkle et al. 2003) was used. Thereafter, we performed optimum extraction of the spectra to improve the signal-to-noise ratio of the data obtained during the aperture extraction (Horne 1986), and removal of telluric and solar features.

Immediately after spectroscopic acquisition, photometric J, H, and Ks measurements were performed. Two imaging sets, each consisting of five frames per filter, in particular were acquired. The S27 camera with a field of view of 28″ × 28″ and a scale of 27.15 mas/pixel was used. Integration time was 120 s in all the filters. The observations were performed using the jitter-imaging technique (NACO_img_obs_AutoJitter template), that is, by applying telescope offsets between frames. The data were reduced using the MIDAS package. After sky subtraction and flat-fielding of the individual frames in the stack, a determination of the offsets between the frames was performed. This allowed us to align each frame on the target and consider the median of all individual frames in the stack. The magnitude of (47171) 1999 TC_{36} was measured on the median frame using classical aperture photometry. Because of the faintness of TNOs, the aperture correction technique is generally used to avoid the significant contribution from the sky background (Barucci et al. 2000). The basis of this method is that the photometric measurement is performed by using a small aperture of similar size to the seeing

Table 2. Results of the visible and infrared photometric observations of the unresolved binary system (47171) 1999 TC_{36}.

Date	UT	Instr.	V	I	$V-I$	J	H	Ks	$J-H$	$H-Ks$
12 Oct. 2006	04:34	NACO				18.24 ± 0.06	17.99 ± 0.08	17.94 ± 0.06	0.25 ± 0.10	0.05 ± 0.10
12 Oct. 2006	05:14	NACO				18.31 ± 0.06	17.99 ± 0.09	17.96 ± 0.05	0.32 ± 0.11	0.03 ± 0.10
09 Nov. 2006	00:58	ISAAC				18.17 ± 0.07	17.85 ± 0.07	17.79 ± 0.08	0.32 ± 0.10	0.06 ± 0.11
09 Nov. 2006	00:58	FORS1	20.25 ± 0.03	18.99 ± 0.03	1.26 ± 0.04					

Date of the observations, UT relative to the beginning of the photometric acquisition sequence and VLT instrument are reported. Photometric results in the filters V, I, J, H, and Ks together with the $V-I$, $J-H$, and $H-Ks$ colors are reported. Photometric results acquired with ISAAC and FORS1 are discussed in detail in Demeo et al. (2009).

disk, and calibrating the aperture effect using nearby field stars (Doressoundiram et al. 2008). The reference stars need to be in the target field since the AO correction of the reference star must be identical to that of the target, otherwise a systematic error is introduced. Because of the absence of stars in the target field, we did not use the aperture correction technique for the magnitude determination of (47171) 1999 TC_{36}. The aperture photometry was completed by the construction of a growth profile (total flux versus aperture size) of the object from its center. The starting point of the plateau of this profile provided the photometric aperture. In Table 2, we present the magnitudes of (47171) 1999 TC_{36} measured on the median frame of each stack of data, and corrected for both the zero point and airmass. Magnitude errors were estimated to be the square root of the quadratic sum of the photometric and calibration (zero point) errors. The error associated with the flat-field was not considered, in the sense that each image was assumed to be perfectly flat-fielded. The zero points of the photometric calibration were measured from observations of S677-D and S840-F from the LCO/Palomar NICMOS list of photometric standards (Persson et al. 1998).

2.2. SINFONI observations

The near-infrared integral field spectrograph SINFONI is installed at the 8 m "Yepun" ESO-VLT facility at the Paranal Observatory in Chile. The instrument is equipped with an infrared detector of 2048×2048 pixels Hawaii 2RG. The observation was completed with the H+K grating, at a spectral resolution of about 1500, allowing us to obtain in a single observation a spectrum between 1.5 and 2.4 μm. The field of view is $8'' \times 8''$. The observations were performed in excellent sky conditions. The circumstances of observations are reported in Table 1.

SINFONI slices the field of view into 32 image-slitlets, which are redirected toward the grating and then reimaged onto the detector. The reduction was performed using the SINFONI pipeline version 1.6. The pipeline accounts for the entire correction procedures automatically and we followed the procedure described in Alvarez-Candal et al. (2007). In short, the pipeline uses a set of nights and static calibrations to account for flat-fielding, wavelength calibration, and sky-subtraction. Finally, it combines the individual cubes to compute the final science cube. The cube includes spatial information (x and y axes), while the spectral information is displayed along the z axis. The spectrum is then extracted using QFitsView (developed by the Max-Plank-Institut für extraterrestrische Physik). The extraction is performed by integrating the flux over an aperture of about $1''$-radius, centered on the photometric center.

The spectrum of (47171) 1999 TC_{36} was then divided by the spectra of the corresponding solar analog (see Table 1), and cleaned as described in Alvarez-Candal et al. (2007). The spectrum was finally smoothed using a running box, a step that provided a final spectral resolution of about 100 and also increased the signal-to-noise ratio.

2.3. ISAAC observations

We used ISAAC to obtain the near-infrared photometry (Demeo et al. 2009) and the J-band spectroscopy from 1.1 to 1.4 μm. We used the short wavelength (SW) mode with a slit of $1''$ width and a spectral resolution of about 500. The observations were completed by nodding the object along the slit by $10''$ between two positions A and B. Following the procedure described by Barucci et al. (2002), the A and B images were subtracted and combined using MIDAS. The wavelength calibration was performed using xenon and argon lamp spectral lines. The object spectrum was divided by the spectrum of solar analog HD 2966 observed at similar airmass (see Table 1) to correct from telluric lines and remove the Sun's contribution to the spectrum, allowing us also to obtain the relative reflectance spectrum of the target. This final J-band spectrum was smoothed using a median filtering to reach a spectral resolution of about 100, to improve the signal-to-noise ratio.

3. Observational results

Figure 1 shows the relative reflectance spectrum acquired with ISAAC (solid line) in J-band and SINFONI (dashed line) in H- and K-bands, normalized to 1 around 1.25 μm. The ISAAC and SINFONI spectra were adjusted using the photometric $J-H$ color (diamonds) determined by the ISAAC instrument on 9 November 2006 (Demeo et al. 2009) and reported in Table 2. It is possible to verify the good agreement between the spectral slope of the target and the $J-Ks$ color (diamond), because the H+K grating of SINFONI covers the complete wavelength range from 1.5 to 2.4 μm. After the SINFONI and ISAAC spectra are combined using the $J-H$ color, the photometry performed in Ks filter is then used only as a check of the spectral slope. The spectrum obtained with NACO instrument (dashed-dot line) almost one month earlier along the wavelength range (1.1–1.7) μm, normalized to 1 around 1.265 μm and shifted by 0.5 in reflectance, is also shown. The spectrum in K-band is not considered because of its poor signal-to-noise ratio. The photometric results (crosses) obtained by averaging the NACO absolute magnitudes of the two different sets of measurements (see Table 2) are overplotted. The NACO spectrum does not show any evidence of particular absorption bands. Even if the quality of NACO spectroscopic measurements is not as high as that obtained by ISAAC and SINFONI, NACO, using the prism S27_P1, provides a spectrum of the target for the complete wavelength range (1.1–1.7) μm, without introducing uncertainties related to the adjustment of the spectra taken in separate filters. The photometric measurements, which are completely independent from the

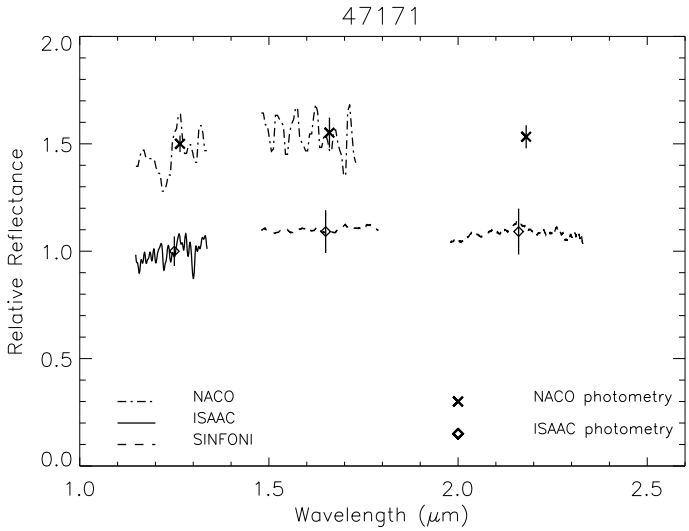

Fig. 1. The relative reflectance spectrum of (47171) 1999 TC_{36} acquired by ISAAC (solid line) in J-band and SINFONI (dashed line) in H- and K-bands is shown. The spectrum obtained with NACO instrument (dashed-dot line) along the wavelength range (1.1–1.7) μm, normalized to 1 around 1.265 μm and shifted by 0.5 in reflectance, is also shown. The normalized photometry in JHKs is overplotted as obtained from ISAAC (diamonds, unit at 1.25 μm) and NACO observations (crosses, unit at 1.265 μm).

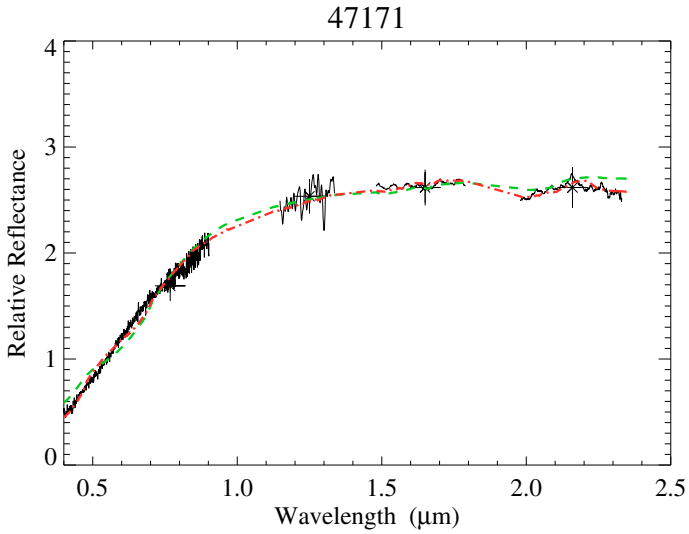

Fig. 2. Spectral reflectance of (47171) 1999 TC_{36} in the V, J, H, and K ranges, normalized to 1 at 0.55 μm. The spectrum has been adjusted using the V, I, J, H, and Ks colors (Demeo et al. 2009), which are represented by crosses with relative errors. The best-fit model (dashed-dot red line) obtained with an intimate mixture of Triton tholin, Titan tholin, serpentine and Triton tholin diluted in crystalline water ice is also shown. The dashed green line represents the best-fit model obtained considering an intimate mixture of Titan tholin, amorphous carbon and Triton tholin diluted in crystalline water ice. (See the electronic version of the Journal for a color version of this figure.)

spectroscopic ones, also allow us to verify the spectral slope of the target in J- and H-bands. Hence, the agreement inside the error bars between NACO photometric and spectroscopic observations confirms the validity of these measurements.

The spectral behaviour of (47171) 1999 TC_{36} recorded with NACO instrument in J- and H-bands is similar to that obtained by combining ISAAC and SINFONI spectroscopic observations. The colors $J - H$ and $H - K$s obtained with NACO and ISAAC are also in agreement to within one standard deviation. All the presented photometric and spectroscopic observations are related to the unresolved binary system (Trujillo & Brown 2002). However, since the magnitude contrast equals 2.14 ± 0.02 mag (Stansberry et al. 2006), these observations are dominated by the primary component. Since the rotational motion of the primary component is most likely complex and a large error is produced after extrapolating the period of 6.21 ± 0.02 h, determined by Ortiz et al. (2003) (0.06 mag of amplitude), to 27 days, it is impossible to relate unambiguously our spectra to specific rotational phases of this component.

Figure 2 shows our ISAAC and SINFONI spectroscopic observations combined with the visible spectrum obtained by FORS1 on 9 November 2006 (see Table 1). The different spectral ranges have been adjusted using the V, I, J, H, and Ks photometric colors (Demeo et al. 2009) and converted into reflectivity using the solar colors given by Hardorp (1980) and Campins et al. (1985). The target spectrum presents a positive spectral slope in the visible range characterized by a spectral gradient S equal to 37.3 ± 0.7%(0.1 μm)$^{-1}$ (Alvarez-Candal et al. 2008) and two possible absorption features around 2.0 and 2.3 μm.

4. Modeling

To extract information about the surface composition of the Plutino (47171) 1999 TC_{36}, the radiative transfer model of Hapke (Hapke 1993) was used to derive the best-fit model of the relative reflectance spectrum of the target, shown as a dashed-dot red line in Fig. 2. This was accomplished by using an intimate mixture of 1% of Triton tholin (optical constants from Khare et al. (1994)) with 5 μm grains, 1% of Titan tholin (optical constants from Imanaka et al. 2004) with 5 μm grains, 97% of serpentine with 336 μm grains, and 1% of Triton tholin diluted in crystalline water ice (H_2O:Tr) with 5 μm grains. The concentration of Triton tholin in crystalline water ice was 45%. Tholins are the most suitable candidates for reproducing the spectral slope of the target up to 1 μm. Serpentine together with water ice, is a good candidate for reproducing the possible feature at 2.0 μm in the target spectrum and exhibits, instead of water ice, an absorption at 2.3 μm. Difficulties in fitting the target spectral slope in the visible range arise when considering areal instead of intimate mixture. Using Triton tholin diluted in crystalline water ice, we can improve the fit of the red slope in the visible region. The optical constants of crystalline water ice were obtained by combining those of Grundy & Schmitt (1998) for the range (0.96–2.74) μm at 40 K with the optical constants from Warren (1984) and Roush (1996) for the ranges (0.30–0.88) μm and (0.88–0.96) μm, respectively. The optical constants used for serpentine are those calculated by Roger Clark in the range (0.3–2.5) μm (private communication). An albedo value of 7% at 0.55 μm was assumed (Stansberry et al. 2008). Isotropical scattering was hypothesized, while the values assumed for surface roughness (θ) and compaction parameter (h) were 0° and 0.05 (a lunar-like surface), respectively. The best-fit model was obtained by considering the grain size and concentration of each surface terrain in the mixture as free parameters, iteratively modified by means of a χ^2 minimization algorithm (Levenberg-Marquardt least-squares minimization) until a best-fit model description of the observations was achieved. This model may not be a unique solution and depends on the surface components considered.

Previous spectroscopic analysis (Dotto et al. 2003) considered the presence of tholins, water ice, and amorphous carbon

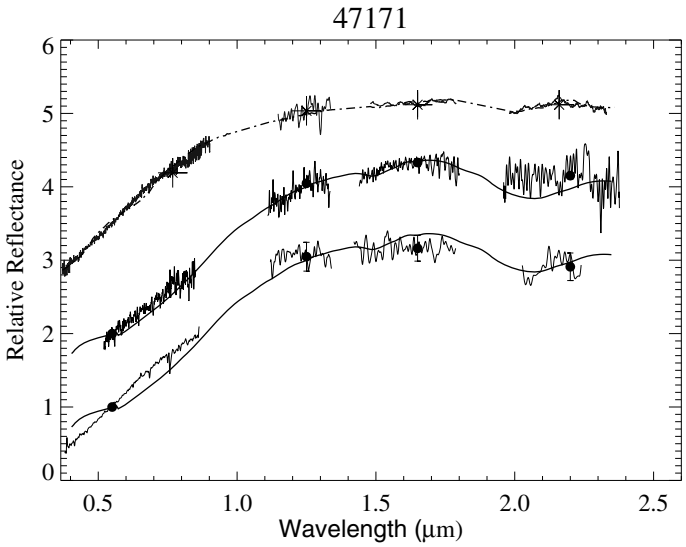

Fig. 3. Relative reflectance spectrum of (47171) 1999 TC_{36} obtained in 2001 by Dotto et al. (2003) (*bottom*), in 2003 by Merlin et al. (2005) (shifted by 1 unit in reflectance) and in 2006 (this work) (shifted by 2.5 unit in reflectance). The two continuous solid lines represent the modeling suggested by Dotto et al. (2003), while in dashed-dot line is shown the best-fit modeling proposed in this work (see dashed-dot red line in Fig. 2).

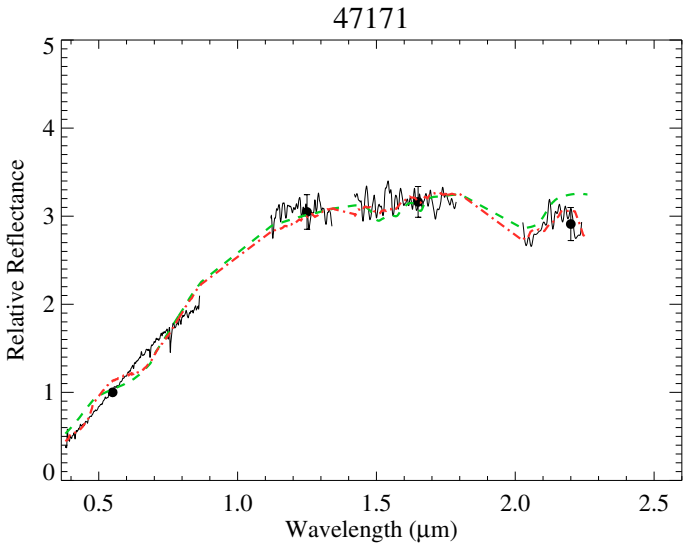

Fig. 4. Spectral reflectance of (47171) 1999 TC_{36} presented by Dotto et al. (2003). Overplotted are our models for these observations. The best-fit model, obtained with an intimate mixture of Titan tholin, serpentine, and Triton tholin diluted in crystalline water ice is shown in red dashed-dot line. The green dashed line represents the best-fit model obtained considering an intimate mixture of Titan tholin, amorphous carbon, and Triton tholin diluted in crystalline water ice. (See the electronic version of the Journal for a color version of this figure.)

on the surface of (47171) 1999 TC_{36}. The tentative best-fit model of (47171) 1999 TC_{36} spectrum that was obtained by considering amorphous carbon instead of serpentine, and no pure Triton tholin is evident in the dashed green line in Fig. 2. This was accomplished with an intimate mixture of 30% of Titan tholin with 5 μm grains, 44% of amorphous carbon (optical constants from Zubko et al. 1996) at 5 μm grains, and 26% of H_2O:Tr with 5 μm grains. The concentration of Triton tholin in crystalline water ice is 49%. By considering serpentine instead of amorphous carbon in the mixture, we are able to improve the best-fit solution, reducing the χ^2 by 5%.

5. Comparison with published results

Dotto et al. (2003) combined near-infrared spectroscopic observations, obtained with the ISAAC instrument on 9 and 10 of September 2001, with the visible spectrum acquired by Lazzarin et al. (2003) with the FORS1 instrument on 15 October 2001. The spectra were adjusted using the photometric B, V, R, I, J, H, and Ks colors obtained on September and October 2001. Figure 3 shows the reflectance spectrum presented by Dotto et al. (2003) together with the photometric colors and the modeling proposed. The modeling solution consists of 57% of Titan tholin, 25% of ice tholin, 10% of amorphous carbon, and 8% of water ice (see solid continuous line). In the same panel, we show, shifted by 1 unit in reflectance, the visible and near-infrared spectra obtained on October 2003 by Merlin et al. (2005), combined by considering the color indices $J-H$ and $J-K$ measured on October 2003 and the $V-J$ color given by Dotto et al. (2003). The reflectance spectrum proposed by Merlin et al. (2005) is compared with the same modeling solution given by Dotto et al. (2003). To correlate the 2001 and 2003 observations with those acquired in 2006, the FORS1-ISAAC-SINFONI observations together with the best-fit modeling proposed in this work, are shown in the same panel, shifted by 2.5 unit in reflectance.

The reflectance spectra acquired on 2001 and 2003 exhibit similar spectral behaviour. As found by Merlin et al. (2005), the colors $J-H$ and $J-K$ obtained on 2003 and 2001 agree to within one standard deviation. The surface modeling proposed by Dotto et al. (2003) also reproduces well the 2003 observations. The 2006 reflectance spectrum compiled in this work differs from that acquired in 2001 and 2003. This difference can be quantified in terms of photometric colors or spectroscopic modeling.

Comparing the photometric colors reported in Table 2 with those obtained by Dotto et al. (2003), it is possible to conclude that the colors $V-I$ and $V-J$ decreased by 0.07 mag and 0.2 mag, respectively. The colors $J-H$ and $H-K$ instead agree to within one standard deviation.

To perform a comparison in terms of surface composition between the 2001 and 2006 data, the Hapke radiative transfer model applied to the 2006 observations (Sect. 4) was also applied to the 2001 data. This approach guaranteed a consistent comparison between the retrieved compositions of the target. Figure 4 shows the relative reflectance spectrum of (47171) 1999 TC_{36} presented by Dotto et al. (2003) together with our best-fit model for these observations, obtained using the same surface components adopted for the modeling of the 2006 data. The dashed green line represents a three terrain unit model consisting of 38% Titan tholin (10 μm grains), 27% amorphous carbon (9 μm grains), and 35% H_2O:Tr (12 μm grains), with 18% of Triton tholin diluted in H_2O. The best-fit model acquired using serpentine instead of amorphous carbon is shown in dashed-dot red line. This model consists of in particular 10% Titan tholin (13 μm grains), 85% serpentine (138 μm grains), and 5% H_2O:Tr (8 μm grains) with 39% of Triton tholin diluted in H_2O. Both models were obtained with the same conditions as those retrieved for the 2006 data. The evidence that serpentine provides a closer fit than amorphous carbon not only for the 2006 observations (Sect. 4) but also for the 2001 data strengthens the presence of this element on the surface of the target.

The modeling analysis of the 2006 and 2001 observations also revealed that the surface composition of the target has changed.

The described spectral behaviour could be due to either time or spatial variations. Although time variations are possible (Protopapa et al. 2008), we consider them less probable because the target surface is volatile-free and interactions between the surface and atmosphere cannot be considered. It is more probable that the surface portion of (47171) 1999 TC_{36} observed by Dotto et al. (2003) and Merlin et al. (2005) is not identical to that observed in 2006. However, it is difficult to identify the different longitudes observed in 2001, 2003, and 2006 because the rotation period of the target is not known to sufficient accuracy to allow us link our spectroscopic measurements to specific rotational phases of the target. Surface heterogeneities have already been observed at the surface of several TNOs such as 1996 TO_{66} (Brown et al. 1999), 38628 Huya, and 47932 2000 GN_{171} (de Bergh et al. 2004) maybe due to partial resurfacing by non-disruptive collisions and/or cometary activity (Merlin et al. 2005).

Acknowledgements. The authors of this paper would like to thank Hermann Boehnhardt for his important help in the discussion of the presented results. Important contributions to this work were also made by Cristina dalle Ore, who provided optical constants required for the modeling analysis. We thank the referee of this paper, Jean-Marc Petit, for his important comments and suggestions.

References

Alvarez-Candal, A., Barucci, M. A., Merlin, F., Guilbert, A., & de Bergh, C. 2007, A&A, 475, 369
Alvarez-Candal, A., Fornasier, S., Barucci, M. A., de Bergh, C., & Merlin, F. 2008, A&A, 487, 741
Barucci, M. A., Romon, J., Doressoundiram, A., & Tholen, D. J. 2000, AJ, 120, 496
Barucci, M. A., Boehnhardt, H., Dotto, E., et al. 2002, A&A, 392, 335
Barucci, M. A., Cruikshank, D. P., Dotto, E., et al. 2005, A&A, 439, L1
Barucci, M. A., Merlin, F., Dotto, E., Doressoundiram, A., & de Bergh, C. 2006, A&A, 455, 725
Barucci, M. A., Brown, M. E., Emery, J. P., & Merlin, F. 2008, Composition and Surface Properties of Transneptunian Objects and Centaurs, The Solar System Beyond Neptune, 143
Brown, M. E. 2008, The Largest Kuiper Belt Objects, The Solar System Beyond Neptune, 335
Brown, M. E., & Calvin, W. M. 2000, Science, 287, 107
Brown, R. H., Cruikshank, D. P., & Pendleton, Y. 1999, ApJ, 519, L101
Brown, M. E., Barkume, K. M., Blake, G. A., et al. 2007a, AJ, 133, 284
Brown, M. E., Barkume, K. M., Ragozzine, D., & Schaller, E. L. 2007b, Nature, 446, 294
Campins, H., Rieke, G. H., & Lebofsky, M. J. 1985, AJ, 90, 896
Cruikshank, D. P., Imanaka, H., & Dalle Ore, C. M. 2005, Adv. Space Res., 36, 178
de Bergh, C., Boehnhardt, H., Barucci, M. A., et al. 2004, A&A, 416, 791
Demeo, F. E., Fornasier, S., Barucci, M. A., et al. 2009, A&A, 493, 283
Doressoundiram, A., Boehnhardt, H., Tegler, S. C., & Trujillo, C. 2008, Color Properties and Trends of the Transneptunian Objects, The Solar System Beyond Neptune, 91
Dotto, E., Barucci, M. A., Boehnhardt, H., et al. 2003, Icarus, 162, 408
Dumas, C., Merlin, F., Barucci, M. A., et al. 2007, A&A, 471, 331
Fornasier, S., Doressoundiram, A., Tozzi, G. P., et al. 2004, A&A, 421, 353
Grundy, W. M., & Schmitt, B. 1998, J. Geophys. Res., 103, 25809
Hapke, B. 1993, Theory of reflectance and emittance spectroscopy, Topics in Remote Sensing (Cambridge, UK: Cambridge University Press)
Hardorp, J. 1980, A&A, 91, 221
Hinkle, K. H., Wallace, L., & Livingston, W. 2003, in BAAS, 35, 1260
Horne, K. 1986, PASP, 98, 609
Imanaka, H., Khare, B. N., Elsila, J. E., et al. 2004, Icarus, 168, 344
Jewitt, D. C., & Luu, J. 2004, Nature, 432, 731
Khare, B. N., Sagan, C., Heinrich, M., et al. 1994, in BAAS, 26, 1176
Lazzarin, M., Barucci, M. A., Boehnhardt, H., et al. 2003, AJ, 125, 1554
Licandro, J., Pinilla-Alonso, N., Pedani, M., et al. 2006, A&A, 445, L35
Merlin, F., Barucci, M. A., Dotto, E., de Bergh, C., & Lo Curto, G. 2005, A&A, 444, 977
Olkin, C. B., Young, E. F., Young, L. A., et al. 2007, AJ, 133, 420
Ortiz, J. L., Gutiérrez, P. J., Casanova, V., & Sota, A. 2003, A&A, 407, 1149
Persson, S. E., Murphy, D. C., Krzeminski, W., Roth, M., & Rieke, M. J. 1998, AJ, 116, 2475
Protopapa, S., Boehnhardt, H., Herbst, T. M., et al. 2008, A&A, 490, 365
Roush, T. L. 1996, in Lunar and Planetary Institute Conference Abstracts, 27, 1107
Stansberry, J., Grundy, W., Brown, M., et al. 2008, Physical Properties of Kuiper Belt and Centaur Objects: Constraints from the Spitzer Space Telescope, The Solar System Beyond Neptune, 161
Stansberry, J. A., Grundy, W. M., Margot, J. L., et al. 2006, ApJ, 643, 556
Tegler, S. C., Grundy, W. M., Romanishin, W., et al. 2007, AJ, 133, 526
Tegler, S. C., Grundy, W. M., Vilas, F., et al. 2008, Icarus, 195, 844
Trujillo, C. A., & Brown, M. E. 2002, IAU Circ., 7787, 1
Trujillo, C. A., Brown, M. E., Barkume, K. M., Schaller, E. L., & Rabinowitz, D. L. 2007, ApJ, 655, 1172
Warren, S. G. 1984, Appl. Opt., 23, 1206
Zheng, W., Jewitt, D., & Kaiser, R. I. 2008, ArXiv e-prints, 801
Zubko, V. G., Mennella, V., Colangeli, L., & Bussoletti, E. 1996, MNRAS, 282, 1321